Sains Malaysiana 53(9)(2024): 3125-3134
http://doi.org/10.17576/jsm-2024-5309-17

Methyl Orange Dye Removal by Dimethylamine Functionalized Graphene Oxide

(Penyingkiran Pewarna Oren Metil oleh Dimetilamina Grafin Oksida Berfungsi)

SEW HUI JUEN, NOOR NAZIHAH BAHRUDIN, NUR AMILAH FADLINA BASRI & MOHD HANIFF WAHID*

Department of Chemistry, Faculty of Science, Universiti Putra Malaysia, 43400 UPM Serdang, Selangor, Malaysia

Received: 18 April 2024/Accepted: 11 July 2024

ABSTRACT

Graphene oxide (GO) functionalized with dimethylamine (DMA) was successfully prepared using a facile technique. GO was first synthesized using the modified Hummers method, followed by chemical functionalization with DMA in the presence of an electrophilic linker, i.e., epichlorohydrin (ECH). FTIR analysis of the end product ascertains the successful synthesis of GO as well as its functionalization with DMA. Typical characteristic peaks attributed to GO and DMA are clearly discernible in the spectrum. The effect of pH, adsorbent dosage, dye concentration, and contact time towards methyl orange (MO) dye removal was studied and reported herein. In summary, enhanced adsorption of methyl orange was observed for DMA functionalized GO compared to GO alone. 90% removal was observed with 10 mg/L of MO concentration, pH = 2 at temperature 25 °C and 5 mg of adsorbent. Modelling study shows that the pseudo-second-order kinetic model and Freundlich isotherm model provide better fitness to the experimental data.

Keywords: Adsorption; dimethylamine; graphene oxide; methyl orange

ABSTRAK

Grafin oksida (GO) difungsikan dengan dimetilamina (DMA) telah berjaya disediakan dengan menggunakan teknik yang mudah. Pada permulaan, sintesis GO telah dilaksanakan menggunakan teknik Hummers terubah suai, diiringi oleh pemfungsian kimia dengan DMA dengan kehadiran linker elektrofilik, epiklorohidrin (ECH). Analisis FTIR ke atas produk membuktikan keberhasilan sintesis GO dan juga pemfungsian dengan DMA. Puncak tipikal GO dan DMA kelihatan jelas di dalam spektra. Kesan pH, dos penjerap, kepekatan pewarna dan masa sentuh terhadap penyingkiran pewarna metil jingga (MO) telah dikaji dan dilaporkan di sini. Secara keseluruhannya, peningkatan penjerapan metil jingga dapat disaksikan bagi penjerap GO berfungsian DMA berbanding GO sahaja. 90% penyingkiran telah diperhatikan dengan kepekatan MO 10 mg/L, pH = 2 pada suhu 25 °C dan 5 mg bahan penjerap. Kajian model kinetik menunjukkan bahawa model pseudo-tertib-kedua dan isoterma Freundlich memberikan keserasian yang lebih kepada data uji kaji.

Kata kunci: Dimetilamina; grafin oksida; metil jingga; penjerapan

INTRODUCTION

Besides the rapid growth of the world population, industrialization and unplanned urbanization, agricultural practices as well as excessive use of chemicals have brought detrimental effect to the environment (Hanafi & Sapawe 2020). Once contaminants are released into the water stream either directly or indirectly without sufficient treatment, water pollution results. The presence of pollutants on the surface or subsurface of water not only harms the environment but also leads to water borne diseases. Among the various types of pollutants, one of them is industrial dyes which comprise the largest group of organic compound-based contaminants and are a major contributor to environmental problems (Hanafi & Sapawe 2020).

Dyes, unlike most organic compounds, exhibit colour due to the presence of chromophore structure made up of extended conjugated system of π-electrons, containing groups with an electron acceptor or donor that may absorb light in the visible range (400 - 700 nm) (Tang, Lo & Kan 2018). They are widely used in industries such as colouring agents in textile or leather, printing, paper manufacturing, pharmaceutical and food processing industries (Hanafi & Sapawe 2020). Dyes usually have complex aromatic molecular structures, which make them more stable and difficult to biodegrade (Amin 2008). Furthermore, due to their high solubility, it is difficult to remove them by conventional treatment facilities (Hanafi & Sapawe 2020; Vijayaraghavan, Won & Yun 2009).

Currently available water treatment techniques used to remove dyes from industrial effluents includes biological treatment, coagulation, sedimentation, adsorption, advanced oxidation process (AOPs), and membrane separation (Gupta 2009). The treatments have their own advantages and disadvantages, nevertheless adsorption appears to be the most attractive of all methods owing to it's simple in design, easy to operate, low operation cost and free from generation of toxic by-products (Amin 2008).

To date, various adsorbents are being used for dye removal from aqueous solutions, such as activated carbon, zeolites, silica gel, alumina, and graphene nanosheets. Given the large modifiable surface functional groups and relatively high mechanical strength, GO features as an ideal adsorbent for a plethora of applications such as water purification, gas separation, and heavy metal removal (Kyzas, Deliyanni & Matis 2014; Tapouk et al. 2019). Nevertheless, modification of GO with functional groups may further enhance its selectivity and adsorption capacity. Herein, GO was functionalized with dimethylamine using a simple technique and its ability to remove methyl orange dye from aqueous solution was studied.

MATERIALS AND METHODS

MATERIALS

Graphite powder and dimethylamine (DMA) were purchased from Sigma-Aldrich, USA. Sulphuric acid (H_2SO_4, 95-98%) and phosphoric acid (H_3PO_4, 85%) used in GO synthesis were purchased from Chemiz. Potassium permanganate ($KMnO_4$) and hydrogen peroxide (H_2O_2) were purchased from Qrec (Malaysia). Hydrochloric acid (HCl, 37%) and epichlorohydrin (ECH) were purchased from R&M Chemicals. Methyl orange (MO, $C_{14}H_{14}N_3NaO_3S$) was obtained from BDH Chemicals Ltd (Poole, England). Sodium hydroxide (NaOH) was purchased from Merck (Whitehouse Station, New Jersey). Distilled water used throughout this project is for dilution and cleaning purposes.

SYNTHESIS OF GO-ECH-DMA

Synthesis of GO-ECH-DMA was carried out following the method reported by Tapouk et al. (2019) with slight modifications. GO was first prepared from graphite flakes using the modified Hummers' method as described in previous works (Marcano et al. 2010; Pohan et al. 2021). 0.3 g of synthesized GO was dispersed in 300 mL of distilled water. The GO suspension was subjected to sonication for 30 min to ensure a homogenous dispersion of GO. Next, while stirring, excess amount of NaOH was added to the GO solution for the deprotonation step. Upon complete dissolution, 10 mL of ECH was added dropwise and the mixture was left to stir for 3 h. 3 M of HCl was then added to neutralize the solution. Product was collected through centrifugal washing by centrifuging at 14,000 rpm for 10 min and the process was repeated 4 times. After each washing cycle, the supernatant was discarded and replaced with fresh distilled water.

To obtain GO-ECH-DMA, 100 mg of GO-ECH were mixed in 250 mL of distilled water and subjected to sonication at 40 °C for 20 min to attain a homogenous solution. The pH was adjusted to pH 12 by adding 1.5 M NaOH. Next, 1 mL of DMA was added dropwise to the GO-ECH solution. The mixture was then refluxed at 60 °C for 3 h. After reflux, the product was centrifuged at 14,000 rpm for 15 min and the product was washed with distilled water to eliminate impurities and unreacted chemicals. The final product GO-ECH-DMA was collected and freeze-dried prior to characterization and adsorption studies.

CHARACTERIZATION

Functional group elucidation via Fourier-transform infrared (FTIR) spectra analysis was performed using an Invenio R FTIR spectrometer (Bruker) equipped with an attenuated total reflectance (ATR) diamond crystal. FTIR spectra were recorded from 4000 to 400 cm^{-1} at 4 cm^{-1} resolution. X-ray diffraction (XRD) analysis was carried out using a Shimadzu 6000 x-ray diffractometer. Surface morphology of the samples was studied using the scanning electron microscopy (SEM) JEOL JSM 6400 operating under 10 kV accelerating voltage.

DYE REMOVAL STUDIES

The adsorption efficiency of the prepared adsorbent samples was tested against MO dye. The parameters studied were pH (1 - 10), adsorbent dosage (1 – 5 mg), dye initial concentration (10 – 50 ppm) and contact time (0 - 260 min). 2 mg of each sample were weighed and added into separate beakers containing 20 mL of 10 ppm MO solution each. All samples were placed on an orbital shaker and were swirled at 150 rpm for 30 min. After 30 min, the solution was collected using a syringe and filtered before recording its UV-Vis absorbance. The UV-Vis analysis was implemented at λ_{max} = 465 nm. Adsorption capacity, Q_e and removal percentage, R % were then calculated using Equations (1) and (2) consecutively.

$$Q_e: \frac{(C_o - C_e)\,v}{m} \quad (1)$$

$$R\%: \frac{(C_o - C_e)}{C_o}\ x\,100 \quad (2)$$

where C_o is the initial MO dye concentration (ppm); C_e is the equilibrium MO dye concentration (ppm); V is the volume of MO dye solution (L); and m is the dry mass of the adsorbent (g).

POINT OF ZERO CHARGE PH (PH_{PZC}) DETERMINATION

The pH_{pzc} of the adsorbent was investigated using the salt addition method. Samples of 0.025 mg of GO-ECH-DMA were added into 10 mL of 0.01M NaCl solution, respectively. The pH of each solution was adjusted to 3, 6, and 9 by dissolving 0.01M HCl or 0.01M NaOH solution. The pH of the solution was verified using a pH meter. The solution was left for 48 h, and the final pH of the solution was recorded. A graph of pH difference vs. initial pH was plotted.

ADSORPTION ISOTHERMS

Adsorption isotherm models were applied to fit the experimental data in order to better describe the adsorption process. Herein, Langmuir (Lagergren 1898) and Freundlich (Freundlich 1906) isotherm models were used to study and analyse the MO dye adsorption equilibrium by GO-ECH-DMA. Langmuir and Freundlich equations are described by the linearized equations as shown in Equations (3) and (4), respectively.

$$\frac{1}{Q_e} = \frac{1}{Q_{max} K_L} \frac{1}{C_e} + \frac{1}{Q_{max}} \tag{3}$$

$$log\, Q_e = log\, K_f + \frac{1}{n}\, log\, C_e \tag{4}$$

where Q_e is as explained earlier, while Q_{max} refers to the capacity of the adsorbent monolayer (mg/g); K_L is the Langmuir adsorption constant; C_e is the equilibrium concentration of MO solution (mg/L). For Equation (4), K_f is the Freundlich constant; Q_e and C_e is same as above; n is the value indicating the degree of linearity between adsorbate and adsorbent (Lagergren 1898); and refers to equilibrium constant.

ADSORPTION KINETICS

Kinetic studies of an adsorption process were performed by measuring differences in absorbance over time. The absorbance signal was then converted to the amount of dye adsorbed on the solid phase and applied to several kinetic models to determine the best match. In this study, two adsorption reaction kinetic models, pseudo-first order (Ho 1995) and pseudo-second order (Lagergren 1898) kinetic models were evaluated to describe the kinetics data obtained from the adsorption of MO dye on GO-ECH-DMA.

The rate expression for the pseudo-first order adsorption and pseudo-second order adsorption as shown in Equations (5) and (6), respectively.

$$ln\,(Q_e - Q) = ln\, Q_e - k_1 t \tag{5}$$

$$\frac{t}{Q_t} = \frac{1}{k_2 Q_e^2} + \frac{t}{Q_e} \tag{6}$$

where t represents time of reaction (min); Q_e refers to amount of MO adsorbed at equilibrium condition (mg/g); Q_t is the amount of MO adsorbed at time t (mg/g); k_1 is the rate constant of pseudo-first order sorption (min^{-1}); and k_2 is the rate constant pseudo second order kinetic equation ($g/mg\ min^{-1}$).

RESULTS AND DISCUSSION

CHARACTERIZATION

FTIR spectra of all samples are as shown in Figure 1. For GO, GO-ECH, and GO-ECH-DMA samples, a broad absorption band between 3250 and 3650 cm^{-1} were discerned, indicating the presence of hydroxyl groups (Tapouk et al. 2019). Noteworthy mentioning, from GO to GO-ECH intensity of the hydroxyl peak decreased in accordance with the deprotonation of hydroxyl groups and attachment of oxirane moieties onto GO. Nevertheless, the peak regained intensity upon addition of DMA due to an increase in the number of hydroxyl groups resulting from the ring-opening reaction of the epoxy groups.

XRD analysis results of the samples are as shown in Figure 2. Presence of a sharp peak at $2\theta = 10.73°$ in the XRD patterns of GO sample, corresponds to interlayer spacing of 8.24 Å, which is due to oxygen containing functional groups such as carboxylic acid, epoxide and -OH group on the GO surface. After the addition of ECH, the XRD pattern of GO-ECH shows that the reflection peak lowered to $2\theta = 9.35°$, corresponding to an increase in interlayer spacing to 9.45 Å due to the intercalation of functional groups such as epoxide (C-O-C) groups (Tapouk et al. 2019). The reduction and loss of diffraction signal in GO-ECH and GO-ECH-DMA could be attributed to the exfoliation of graphene oxide sheets during synthesis with ECH and DMA, resulting in the loss of solid crystalline structure (Tienne et al. 2022).

The surface morphology of GO and GO-ECH-DMA was also studied using Scanning Electron Microscope (SEM) analysis. SEM images in Figure 3 display the typical thin layered-like structures with wrinkles on the surface, which indicates successful GO synthesis process. Meanwhile, SEM micrograph of GO-ECH-DMA revealed that the latter possessed more wrinkles and defects on the surface (Figure 3(c) & 3(d)). This is consistent with the functionalization process which induces lattice deformation (Tapouk et al. 2019; Zheng et al. 2010).

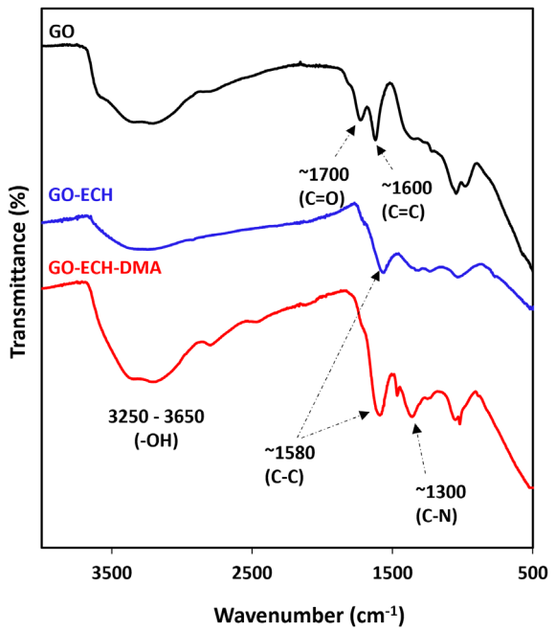

FIGURE 1. IR spectra of GO, GO-ECH and GO-ECH-DMA

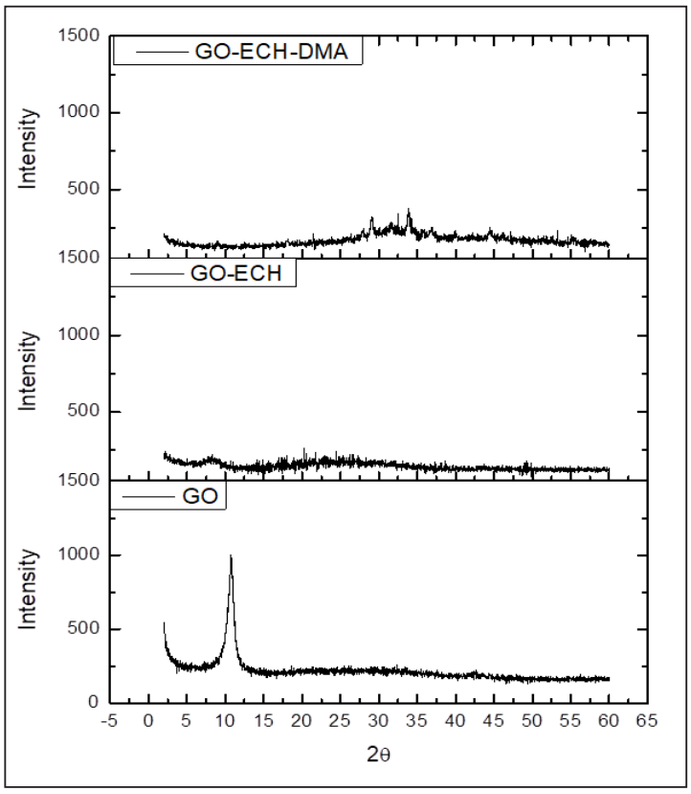

FIGURE 2. XRD diffractograms of GO-GO-ECH and GO-ECH-DMA

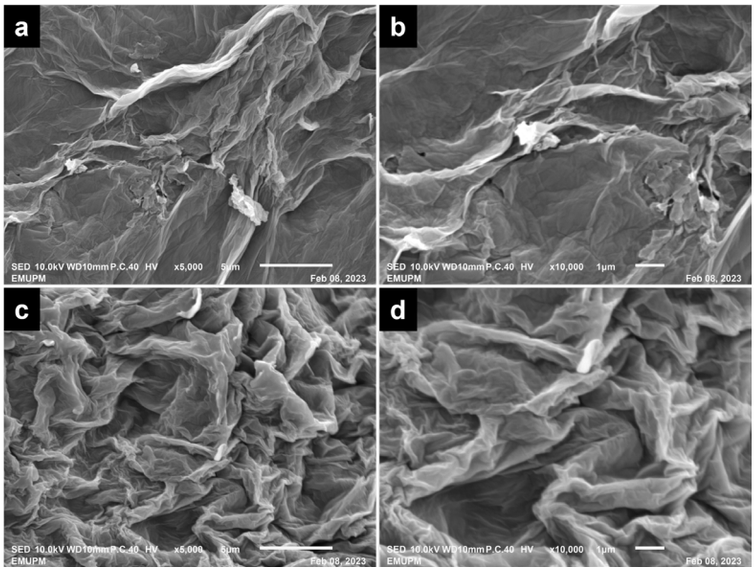

FIGURE 3. SEM micrograph of (a) GO at 5000x magnification, (b) GO at 10000x magnification. (c) GO-ECH-DMA at 5000x magnification, (d) GO-ECH-DMA at 10000x magnification

TABLE 1. Amount of ECH and DMA for different GO-ECH-DMA samples

Sample	Formulation		
	GO (mg)	ECH (mL)	DMA (mL)
1	300	10	3
2	300	10	1
3	300	10	5
4	300	5	3
5	300	15	3
6	300	20	3

OPTIMIZATION OF ADSORBENT

MO dye removal efficiency by pristine GO and GO-ECH-DMA were tested under the conditions of 2 mg of each adsorbent against 20 mL of 10 ppm MO solution each. All samples were placed on an orbital shaker and were subjected to swirling at 150 rpm for 30 min. After 30 min, the solution was collected and filtered prior to UV-Vis analysis. Results obtained are as shown in Figure 4(a). The preliminary test results showed that functionalized GO exhibited a higher removal percentage of MO dye which is 12.1% compared to pristine GO with removal percentage of 7.4%.

The adsorption of MO on GO-ECH-DMA was much more effective compared to GO which can be attributed to the presence of positively charged DMA binding sites that has a higher affinity to adsorb MO dye through the electrostatic attraction of DMA to the negatively charged sulfonate group of the dye. Optimum amount of DMA was studied by fixing the volume of ECH at 10 mL while DMA amount was varied at 1, 3, and 5 mL. Based on the results by GO-ECH-DMA synthesised using different ECH volumeshown in Figure 4(b), MO removal for GO-ECH-DMA with 3 mL DMA is the highest which is 12.13%, while GO-ECH-DMA with 1 mL and 5 mL of DMA adsorbed 2.59% and 9.72% of MO dye, respectively. Next, the volume of ECH was optimized. The volume of DMA was fixed at 3 mL and volume of ECH was varied at 5, 10, 15, and 20 mL and their adsorption performance are as shown in Figure 4(c).Based on the results obtained, GO-ECH-DMA sample synthesized with 15 mL ECH shows the highest adsorption efficiency of MO dye with removal up to 12.69%. While for GO-ECH-DMA synthesized with 5, 10, and 20 mL of ECH,the removal on MO dye is 7.73%, 12.13% and 5.13%, respectively. Therefore, 15 mL ECH and 3 mL of DMA was considered for the preparation of

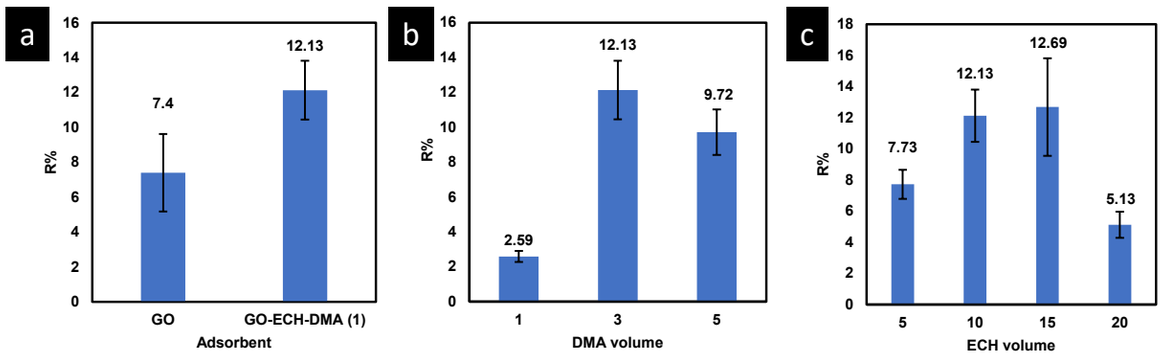

FIGURE 4. (a) Graph of removal percentage of methyl orange by GO and GO-ECH-DMA (1) (b) Removal of methyl orange by GO-ECH-DMA synthesised using different DMA volume (c) Removal of methyl orange

GO-ECH-DMA for the adsorption parameters studies. Summary of the prepared GO-ECH-DMA samples are as shown in Table 1.

BATCH ADSORPTION STUDIES OF MO DYE BY GO-ECH-DMA

The effect of adsorption parameters, i.e., solution pH, adsorbent dose, initial concentration of MO dye and contact time towards MO adsorption were studied. The pH_{pzc} of GO and GO-ECH-DMA was determined using the salt addition method to assess the ideal pH of the solution for MO adsorption. According to Figure 5(a), the surface of GO and GO-ECH-DMA is assumed to be neutrally charged at solution pH 3.0 and 7.5, respectively. When solution pH is lower than pH_{pzc} of the adsorbent, the functional groups on the adsorbent surface are protonated and the overall net charge of the adsorbent surface will be positive. Conversely, in solution with pH higher than pH_{pzc} of the adsorbent, the functional groups are deprotonated. Hence, there is an overall net negative charge on the surface of adsorbent. Ideally, the protonated adsorbents are expected to attract and thus bind with the anionic MO dye.

Based on the pH_{pzc} test, both GO and GO-ECH-DMA were found to be positively charged at solution pH less than 3 (Figure 5(a)). Nevertheless, GO-ECH-DMA material has a higher pH_{pzc} value than pure GO, indicating that it acts as a positively charged species at higher pH values. This suggests that the GO-ECH-DMA will be able to adsorb the MO dye over a wider range of pH values compared to pure GO. The successful grafting of DMA ligands onto the GO surface and is believed to be the reason for this.

The adsorption performance of GO-ECH-DMA was evaluated by determining the adsorbed amount of MO on GO-ECH-DMA from pH 1 to 10 (Figure 5(b)). Noteworthy mentioning, for acidic pH, i.e., pH 1, 2 and 4 the UV-Vis analysis was carried out at λ_{max} = 507 nm. The highest percentage of MO removal from GO-ECH-DMA The dye removal decreases as the pH increases, with a significant decrease from pH 2 to pH 4, and the removal percentage remains low at pH 8-10. The influence of pH on dye adsorption performance is most likely related to the structure of MO dye, which is distinguished by the presence of an azo and a sulfonate group. The MO dye generally forms anions due to the existence of negatively charged sulfonate ions $(SO_3)^{2-}$ when dissolved in water. However, the MO dye is protonated in solutions with pH less than 4. The proton will bind to the N atom in the diazo bond near the sulfonate group, causing the positive charge to delocalize into the benzene ring linked to the dimethylamine group. As a result, at pH less than 4, the MO ion has a negative charge from the sulfonate group and a partially positive charge from the dimethylamine group. The negatively charged sulfonate group will electrostatically be attracted to the positively charged DMA functional group, and the partially positive charge dimethylamine group in MO may react with the negatively charged GO surface that is not grafted with the DMA functional group. While increasing the pH to an alkaline condition reduces adsorption performance, this can be attributed to the competition of excess OH^- with anionic MO dyes for adsorption sites. Similar results were examined by MO adsorption onto wheat straw modified cationic surfactant and MO removal onto methyl ammonium bromide modified extracted cellulose (Lafi et al. 2022; Su et al. 2014).

Another probable reason for the decline of adsorption at high pH is that as pH rises above pH_{pzc}, surface charge of the adsorbent becomes negative hence not favourable for the adsorption of anionic dye molecules. Given that the pH_{pzc} for GO-ECH-DMA is approximately recorded at 7.5, at pH less than 7.5, the adsorbent surface is positively charged. As the acidity increases, the more tendency that the adsorbent surface stays positively charged, and the higher the tendency for MO dye to be adsorbed onto the GO-ECH-DMA surface. Based on the results of the experiments, pH 2 was selected as the optimal pH value and was used in subsequent testing.

The relationship between MO adsorption and GO-ECH-DMA dosage was then investigated by varying the

amount from 1 mg to 5 mg in 20 mL MO dye solution. The pH of MO dye solution was maintained at pH 2, and other parameters such as initial concentration, contact time and temperature were kept constant. The effect of GO-ECH-DMA dosage on MO dye removal percentage is shown in Figure 5(c).

With the increase of GO-ECH-DMA dose from 1 to 3 mg, the increase of removal percentage of MO dye was significantly observed. This can be attributed to the high accessibility of available binding sites on the adsorbent for MO dye adsorption. However, when the GO-ECH-DMA dosage was increased from 4 to 5 mg, the rise in MO dye adsorption shows a slight increase. This could be due to most of the adsorption sites are still vacant while most of the MO dye molecules are already adsorbed onto the surface (Lafi et al. 2022).

The adsorption efficiency of GO-ECH-DMA towards the adsorption of MO dyes was studied by varying initial MO dye concentration and contact time (Figure 5(d)). The amount of MO dye taken up by the GO-ECH-DMA per unit mass increased rapidly from 0 to 30 min of contact time and achieved equilibrium at around 100 min. The adsorption of MO dye showed fast increment for the first 30 min since at the beginning of the MO dye adsorption, the surface of the GO-ECH-DMA adsorbent had a high availability of unoccupied binding sites for MO adsorbate. Thus, the MO dye binds to the surface DMA functional groups on GO-ECH-DMA readily. Meanwhile, after 30 min, due the reduced number of available binding sites, MO dyes began to compete (Lafi et al. 2022). This phenomenon made it difficult for MO ions to bind to the adsorption site, causing the adsorption process to slow down. It was also observed that the initial dye concentration has less effect towards the time taken to reach equilibrium. The maximum amount of MO dye absorbed by GO-ECH-DMA at equilibrium for concentrations of 10, 20, 30, 40, and 50 ppm is 44.56, 81.84, 101.40, 127.68, and 136.48 mg/g, respectively. In brief, the adsorption capacity of GO-ECH-DMA had improved by increasing initial MO dye concentration in the aqueous solution. This could be explained due to the increase of driving force resulting from the concentration gradient (Ghorbani et al. 2008).

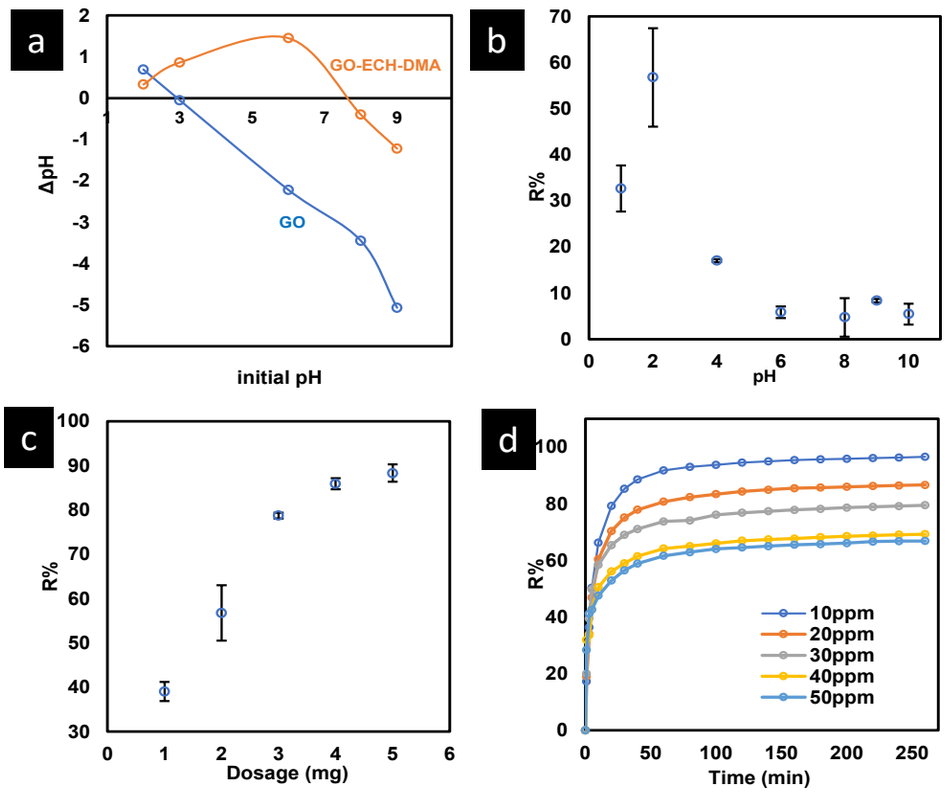

FIGURE 5. (a) The pHpzc of GO and GO-ECH-DMA, (b) Effect of solution pH on the adsorption of methyl orange dye by GO-ECH-DMA, (c) Effect of GO-ECH-DMA dosage on the adsorption of methyl orange dye and (d) Effect of initial MO dye concentration and contact time on MO dye adsorption by GO-ECH-DMA

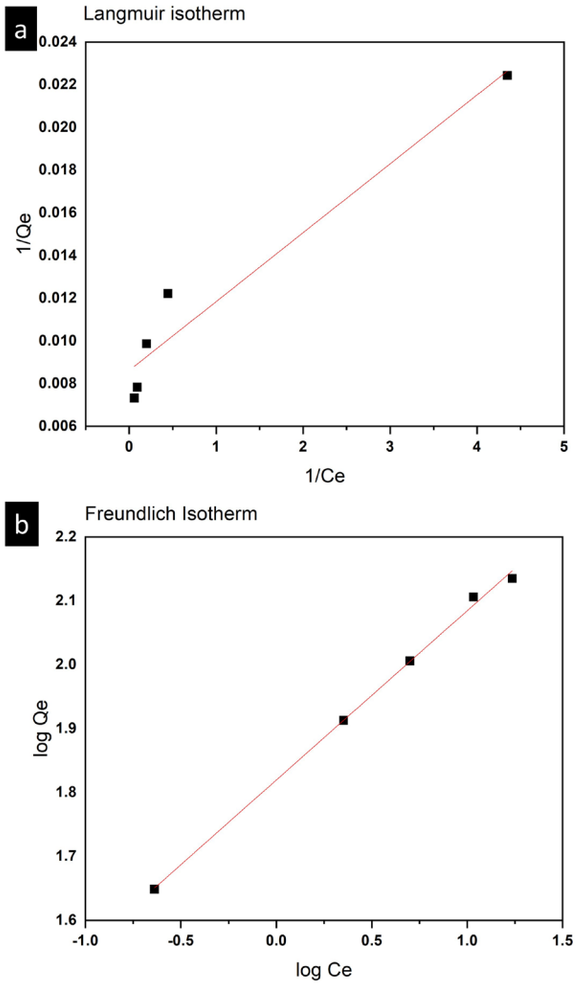

FIGURE 6. Isotherm models for MO removal by GO-ECH-DMA
(a) Langmuir and (b) Freundlich

TABLE 2. Langmuir and Freundlich parameters for adsorption of MO on GO-ECH-DMA

Langmuir			Freundlich		
R^2	K_L	Q_m	R^2	K_F	1/n
0.926	2.688	116.2	0.997	66.0	0.265

TABLE 3. Parameters of Pseudo-first order and Pseudo-second order kinetic model

Pseudo-first order		Pseudo-second order	
k_1	R^2	k_2	R^2
-0.00007	0.922	0.00182	0.999

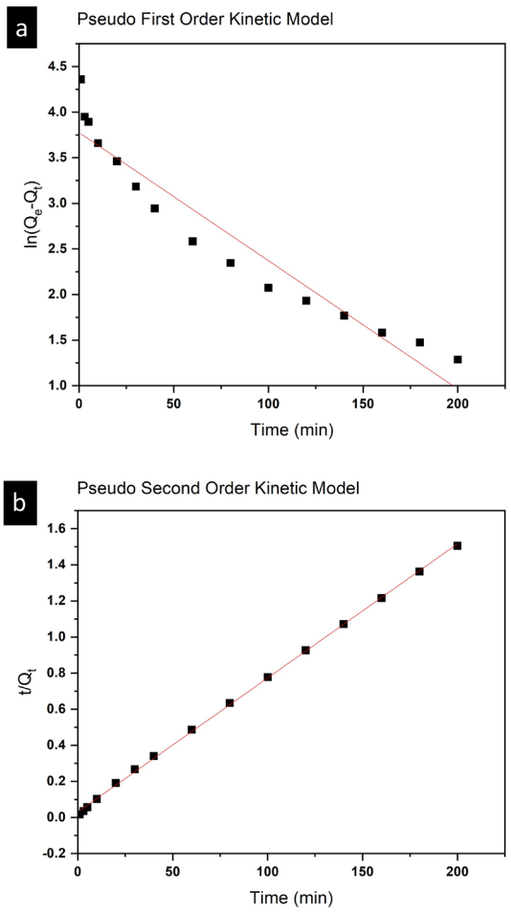

FIGURE 7. Kinetic models for MO removal by GO-ECH-DMA
(a) Pseudo First Order, (b) Pseudo Second Order

ADSORPTION ISOTHERMS

Langmuir and Freundlich isotherm models were both plotted and are shown in Figure 6(a) and 6(b). Table 2 shows the empirical coefficients of each model which was determined from the slope and intercept of the linear plot. Based on Table 2, the experimental data fitted well with the Freundlich isotherm model as the correlation value, R^2, obtained from Freundlich isotherm model is higher than the Langmuir isotherm model and closer to 1, with $R^2 = 0.997$. This thus suggests that the adsorption is better described by the Freundlich model in which the adsorption is heterogenous. According to the calculated equilibrium constant, $1/n = 0.265$, it indicates that the adsorption of MO dye onto GO-ECH-DMA under the studied concentration range is favourable.

ADSORPTION KINETIC MODELLING

A graph of ln (Q_e-Q_t) versus t yields a straight line as shown in Figure 7(a). The value of k_1 and Q_e were then calculated from the slopes and the intercepts of the plot. Similarly, the values of k_2 and Q_e was determined from the slopes ($1/Q_e$) and the intercepts ($1/k_2Q_e^2$) from the linear plot t/Q versus t as shown in Figure 7(b). The pseudo-first order kinetic model assumes that physisorption limits the adsorption rate of the particles onto the adsorbent whereas the pseudo-second order kinetic model considers chemisorption as the rate-limiting mechanism of the process. From Table 3, it is known that the R^2 value for pseudo-second order model ($R^2 = 0.999$) is higher than the R^2 value obtained from pseudo-first order model ($R^2 = 0.922$), thus the experimental data is more fitted to pseudo second order kinetics model.

The chemisorption process involving valence forces, wherein electrons are covalently shared or exchanged between adsorbent and adsorbate, is described by a pseudo-second order kinetic model. In this situation, the molecule may be attracted to the active site rather than any random adsorbent surface's sites, forming first a single layer and possibly other layers via chemisorption.

CONCLUSION

The present study is mainly focused on the removal of MO dye from aqueous solution by GO-ECH-DMA adsorbent. The GO-ECH-DMA was successfully synthesized in this study. The characteristics of GO-ECH-DMA were studied based on the analysis of FTIR, TGA, XRD and pH_{pzc}. Batch adsorption studies were performed under different experimental conditions such as pH, adsorbent dosage, initial concentration of MO dye and contact time to evaluate the adsorption capacities of GO-ECH-DMA adsorbent. The adsorption mechanism and its nature were proposed based on isotherm and kinetic studies.

The result from GO-ECH-DMA optimisation showed that the highest efficiency of adsorption for modified GO to the adsorption of MO dye is the GO-DMA synthesized with 15 mL ECH and 3 mL DMA. The optimal condition for the adsorption of MO dye is observed as pH 2 and adsorbent dosage 5 mg. Experimental data showed better agreement with Freundlich isotherm model and pseudo second order kinetic model, which indicates that the adsorption is heterogeneous and probably involves multilayer adsorption.

ACKNOWLEDGEMENTS

This work has been supported by the Ministry of Higher Education, Malaysia through Fundamental Research Grant Scheme (FRGS) Grant No: FRGS/1/2018/STG01/UPM/02/11.

REFERENCES

Amin, N.K. 2008. Removal of reactive dye from aqueous solutions by adsorption onto activated carbons prepared from sugarcane bagasse pith. *Desalination* 223(1-3): 152-161.

Freundlich, H.M.F. 1906. Over the adsorption in solution. *J. Phys. Chem. A* 57: 385-470.

Ghorbani, F., Younesi, H., Ghasempouri, S.M., Zinatizadeh, A.A., Amini, M. & Daneshi, A. 2008. Application of response surface methodology for optimization of cadmium biosorption in an aqueous solution by *Saccharomyces cerevisiae*. *Chemical Engineering Journal* 145(2): 267-275.

Gupta, V.K. 2009. Application of low-cost adsorbents for dye removal–A review. *Journal of Environmental Management* 90(8): 2313-2342.

Hanafi, M.F. & Sapawe, N. 2020. A review on the water problem associate with organic pollutants derived from phenol, methyl orange, and remazol brilliant blue dyes. *Materials Today: Proceedings* 31: A141-A150.

Ho, Y-S. 1995. Absorption of heavy metals from waste streams by peat. PhD Thesis. University of Birmingham (Unpublished).

Kyzas, G.Z., Deliyanni, E.A. & Matis, K.A. 2014. Graphene oxide and its application as an adsorbent for wastewater treatment. *Journal of Chemical Technology & Biotechnology* 89(2): 196-205.

Lafi, R., Abdellaoui, L., Montasser, I. & Hafiane, A. 2022. Removal of methyl orange from aqueous solution onto modified extracted cellulose from *Stipa tenacissima* L. *International Journal of Environmental Analytical Chemistry* 102(19): 8124-8140.

Lagergren, S. 1898. About the theory of so-called adsorption of soluble substances. *Kungliga Svenska Vetenskapsakademiens Handlingar* 24: 1-39.

Marcano, D.C., Kosynkin, D.V., Berlin, J.M., Sinitskii, A., Sun, Z., Slesarev, A., Alemany, L. B., Lu, W. & Tour, J.M. 2010. Improved synthesis of graphene oxide. *ACS Nano* 4(8): 4806-4814.

Pohan, N.A., Wahid, M.H., Zainal, Z. & Ibrahim, N.A. 2021. Pickering-emulsion-templated synthesis of 3D hollow graphene as an efficient oil absorbent. *RSC Advances* 11(7): 3963-3971.

Su, Y., Jiao, Y., Dou, C. & Han, R. 2014. Biosorption of methyl orange from aqueous solutions using cationic surfactant-modified wheat straw in batch mode. *Desalination and Water Treatment* 52(31-33): 6145-6155.

Tang, A.Y.L., Lo, C.K.Y. & Kan, C. 2018. Textile dyes and human health: A systematic and citation network analysis review. *Coloration Technology* 134(4): 245-257.

Tapouk, F.A., Nabizadeh, R., Nasseri, S., Mesdaghinia, A., Khorsandi, H., Mahvi, A.H., Gholibegloo, E., Alimohammadi, M. & Khoobi, M. 2019. Endotoxin removal from aqueous solutions with dimethylamine-functionalized graphene oxide: Modeling study and optimization of adsorption parameters. *Journal of Hazardous Materials* 368: 163-177.

Tienne, L.G.P., da Silva Candido, L., da Cruz, B. de S.M., Gondim, F.F., Ribeiro, M.P., Simão, R.A., Marques, M. de F.V. & Monteiro, S.N. 2022. Reduced graphene oxide synthesized by a new modified Hummer's method for enhancing thermal and crystallinity properties of poly(vinylidene fluoride). *Journal of Materials Research and Technology* 18: 4871-4893.

Vijayaraghavan, K., Won, S.W. & Yun, Y-S. 2009. Treatment of complex Remazol dye effluent using sawdust-and coal-based activated carbons. *Journal of Hazardous Materials* 167(1-3): 790-796.

Zheng, Q., Geng, Y., Wang, S., Li, Z. & Kim, J-K. 2010. Effects of functional groups on the mechanical and wrinkling properties of graphene sheets. *Carbon* 48(15): 4315-4322.

*Corresponding author; email: mw_haniff@upm.edu.my